ROBOTIC POSE ESTIMATION VIA AN ADAPTIVE KALMAN FILTER USING STATE-VARYING NOISE

Gregory K. Fricke
Mechanical Engineering
& Materials Science
Duke University
Box 90300, Hudson Hall 144
Durham, NC 27708
United States of America
email: gregory.fricke@duke.edu

Dejan Milutinović
Applied Mathematics
& Statistics
University of California at Santa Cruz
Mail Stop SOE2, 1156 High Street
Santa Cruz, CA 95064
United States of America
email: dejan@soe.ucsc.edu

Devendra P. Garg
Mechanical Engineering
& Materials Science
Duke University
Box 90300, Hudson Hall 144
Durham, NC 27708
United States of America
email: dpgarg@duke.edu

ABSTRACT
Swarm robotics offers the promise of enhanced performance and robustness relative to that of individual robots, with decreased cost or time-to-completion for certain tasks. Having many degrees of freedom, the swarm related control and estimation problems are quite challenging, specifically when the solutions involve a large amount of communication among the robots. Under certain sensing modalities, direct measurement of robot orientation may either be not possible or require excessive sensor processing. In this paper, a novel method is presented to vary process noise intensity as a function of an estimated state in order to arrive at the hidden state robot orientation. Experimental results are provided, demonstrating the efficacy of the method as well as the error reduction relative to fixed-noise estimation.

KEY WORDS
collective robotics, pose estimation, kalman filter, stochastic estimation, mobile robotics, differential-drive

1 Introduction

Robotic pose estimation is critical for proper feedback control of robot trajectory. Pose estimation and robot localization have been studied extensively, utilizing methods such as dead-reckoning [1–6], on-board and off-board computer vision [7, 8], environmental sensing [9–11], collective or distributed localization [12, 13], and simultaneous localization and mapping (SLAM) [14] using laser-scanning systems [15, 16], on-board cameras [17], or ultrasonic rangefinders [11]. Most of the above works rely on some variant of the Kalman Filter [18] or Extended Kalman Filter [19].

Dead-reckoning solutions are notoriously susceptible to accumulated error due to modeling errors or unmodeled dynamics such as wheel-slippage or uneven surfaces. The above references include several methods for odometry correction or calibration, all of which require some secondary form of sensing for feedback correction.

Computer vision-based localization systems generally come in two flavors: off-board and on-board. Off-board implementations feature either high-speed sensors with high-complexity pattern recognition and tracking software (requiring extensive computational capability and advanced machine-vision techniques) or simpler vision systems reliant on known configurations or patterns on the robot(s) being tracked (see, e.g., [20, 21]).

On-board solutions rely on feature tracking in the environment, requiring that the environment contains sufficient features to identify and track. Early work required *a priori* known environmental maps or beacon locations [7, 9]; more recent SLAM methods build the environmental map as the robot moves [14, 16]. Similar environmental constraints are placed on laser-scanning- and ultrasonic rangefinder-based SLAM implementations. Additionally, on-board solutions necessarily place significantly higher sensing and computation requirements on the individual robots.

1.1 Problem formulation

This research group, performing research in collective robotics and decentralized formation control, seeks to perform algorithmic development, test, and evaluation in the presence of real-world noise with minimal equipment overhead. As a surrogate for significantly more complex sensing systems on-board the robots, measurements of the system will be made by external position sensors and made available to the individual robots via direct or broadcast wireless communication. Such global information sharing may be considered analogous to the information sharing utilized in [22]. If, for a particular experiment, sensing or communication range is assumed to be limited for individual robots, direct central-computer-to-robot communication could be configured to only report information that the robot would accordingly have access to if the sensing ability were on-board. This type of experimental environment may be called *mixed-simulation testing*, indicating a combination of real and simulated components. Such testbeds are used extensively for validation of complex systems such as spacecraft [23].

The robotic agents forming the basis of the preliminary testbed development are Khepera-II differential drive robots from K-Team. External observations of robots in the testbed are provided by two SICK LMS400 LADAR sensors and an overhead Cognex Insight 5400 industrial machine-vision system. The LADAR sensors provide measurement of the $x-y$ position of multiple agents within the swarm arena. However, due to the nearly uniform cylindrical shape of the Khepera-II robots when viewed from the side, it is not possible to directly measure the agent orientation θ from the range data returned by the LADAR sensors. The vision system has the capability of returning orientation data *provided there are distinguishable features which correlate with the robot orientation* when viewed from above. Measuring the robot orientation in this way requires significant additional processing time, especially in the case of scalable problems related to swarm and cooperative robotics.

In this paper we present an alternative approach in which the orientation of the agent is treated as a hidden variable, and is estimated through observation of the robot motion. The dynamic model of the robot (specifically, the non-holonomicity) is then exploited to appropriately vary the process noise covariance used in the extended Kalman Filter (EKF). Recent papers have discussed covariance variation via fuzzy logic and with dependence on time-step k [11, 24]; the authors of this paper are not aware of prior work utilizing state estimates to vary the covariance.

2 Model Definition

The pose of an individual agent in a swarm is defined by the coordinates $[x, y, \theta]^T$, where x and y are the agent coordinates in a rectangular reference frame, and θ is the orientation angle with $\theta = 0$ lying on the x-axis. The agent posture changes via the agent's on-board control loop, which defines the agent's linear acceleration $\dot{v}$ and angular velocity $\dot{\theta}$. The dynamic model of the robot used in this paper is given in state space form in Eqs.(1-3).

$$X(t) = \begin{bmatrix} x_1 \\ x_2 \\ x_3 \\ x_4 \end{bmatrix} = \begin{bmatrix} x(t) \\ y(t) \\ v(t) \\ \theta(t) \end{bmatrix} \tag{1}$$

$$\mathbf{F}(X(t)) = \begin{bmatrix} f_1 \\ f_2 \\ f_3 \\ f_4 \end{bmatrix} = \begin{bmatrix} v(t)\cos\theta(t) \\ v(t)\sin\theta(t) \\ 0 \\ 0 \end{bmatrix} \tag{2}$$

$$\dot{X}(t) = \begin{bmatrix} \dot{x}(t) \\ \dot{y}(t) \\ \dot{v}(t) \\ \dot{\theta}(t) \end{bmatrix} = \mathbf{F}(X(t)) + \begin{bmatrix} 0 \\ 0 \\ \xi_v(t) \\ \xi_\theta(t) \end{bmatrix} \tag{3}$$

Knowledge of these control inputs $\dot{v}$ and $\dot{\theta}$ would greatly decrease the error in the estimation. In many cases, such as the one described in this paper for an external observer, the control inputs are unknown. For this reason, the control variables $\dot{v}$ and $\dot{\theta}$ are modeled with the zero-mean white noises $\xi_v(t)$ and $\xi_\theta(t)$, respectively. Measurements provided by the vision system and/or LADAR pair are absolute position measurements x_m and y_m assumed to include zero-mean Gaussian-distributed noise $w_x \sim N(0, W_x)$ and $w_y \sim N(0, W_y)$. This measurement model is defined in Eq.(4).

$$\begin{aligned} Z(t) &= \begin{bmatrix} x_m(t) \\ y_m(t) \end{bmatrix} \\ &= \underbrace{\begin{bmatrix} 1 & 0 & 0 & 0 \\ 0 & 1 & 0 & 0 \end{bmatrix}}_{C} X(t) + \begin{bmatrix} w_x \\ w_y \end{bmatrix} \end{aligned} \tag{4}$$

We utilize stochastic signals as a general model of the unknown control signals. The advantage of modeling the unknown control signals as stochastic signals is that we can exploit Kalman filter theory to estimate unknown speed v and angle θ based only on the position measurements x_m and y_m.

We initially assume that the white noise signals that model the control variables are uncorrelated. To establish the baseline, we also assume that they are of constant intensity. In the rest of this paper we will consider the posture estimation based on this constant intensity model as compared to another model in which the noise intensity ξ_θ varies as a function of estimated robot velocity.

The rationale behind the velocity-varying models for estimation lies in the intuition that the largest changes in orientation are likely to be experienced when the velocity v is small. This is due to the observation that for a differential-drive robot, fast orientation changes result from large differences in wheel speeds. For such a system with a limited dynamic range of wheel speeds, the maximum rate of orientation change will occur when the two wheels are each driven at the maximum wheel speed but in opposite directions, resulting in zero linear velocity. At the other extreme, maximum linear velocity is achieved when both wheels are driven at maximum speed in the same direction, resulting in zero angular velocity. Additionally from an observational standpoint, in the limit as velocity goes to zero, changes in x_m and y_m will be zero or undetectable while the orientation may change in range $[0, 2\pi]$.

2.1 Orientation Estimation

Our proposed method is based on the 2nd-order Kalman filter [19] for non-linear systems. Individual agents in the swarm are characterized by the state vector $X = [x, y, v, \theta]^T$, and the continuous state space model is defined by Eqs.(1-3). The Kalman filter is based on two steps: the prediction and the update. The prediction and update step equations are presented below without derivation. Additional details are available in references [18, 19].

In the *prediction step*, the computation of the predicted value $\bar{X}$ of the state vector and its covariance are based on the last estimation $\hat{X}$. Since we are dealing with data that is regularly sampled with sampling period Δt, we use the discrete time version of the 2nd-order filter. The subscript k indicates the iteration step; the predicted state vector at the $k+1$ sample is given by

$$\begin{aligned}\bar{X}_{k+1} &= E_{\hat{X}_k,P}\{X_{k+1}\} \\ &= E_{\hat{X}_k,P}\{X_k + \mathbf{F}(X_k)\Delta t\}\end{aligned} \tag{5}$$

where the expectation is in regard to Gaussian distribution with the mean value $\hat{X}_k$ and corresponding covariance P. Using the Taylor Series expansion up to the second-order terms and including $E_{\hat{X}_k,P}(X_k - \hat{X}_k) = \mathbf{0}$ the above expression can be rewritten as

$$\begin{aligned}\bar{X}_{k+1} = \hat{X}_k + \mathbf{F}(\hat{X}_k)\Delta t + \\ \frac{1}{2}E\left\{\sum_{i=1}^{4}\phi_i(X_k - \hat{X}_k)^T F_i (X_k - \hat{X}_k)\right\}\end{aligned} \tag{6}$$

in which the vectors ϕ_i are: $\phi_1 = [1\ 0\ 0\ 0]^T$, $\phi_2 = [0\ 1\ 0\ 0]^T$, $\phi_3 = [0\ 0\ 1\ 0]^T$, $\phi_4 = [0\ 0\ 0\ 1]^T$ (i.e., typical orthonormal basis vectors of $\Re^4$) and the matrix F_i is

$$[F_i]_{mn} = \frac{\partial^2 f_i(\hat{X}_k)}{\partial x_m \partial x_n}\Delta t,\ m,n = 1,2,3,4. \tag{7}$$

The notation $[\ \cdot\ ]_{mn}$ denotes the element in row m and column n. We can then rewrite Eq.(6) as shown in Eq.(8).

$$\bar{X}_{k+1} = \hat{X}_k + \mathbf{F}(\hat{X}_k)\Delta t + \frac{1}{2}\sum_{i=1}^{4}\phi_i tr\{F_i P_k\} \tag{8}$$

The square matrix P_k denotes the covariance matrix of the state estimate, i.e., $P_k = E\left\{(X_k - \hat{X}_k)^T(X_k - \hat{X}_k)\right\}$. From Eq.(2) and Eq.(7), we obtain $F_3 = F_4 = \underline{0}$, and F_1 and F_2 as defined in Eqs.(9-10).

$$F_1 = \begin{bmatrix}0 & 0 & 0 & 0\\ 0 & 0 & 0 & 0\\ 0 & 0 & 0 & -\Delta t\sin(\theta_k)\\ 0 & 0 & -\Delta t\sin(\theta_k) & -\Delta t v_k\cos(\theta_k)\end{bmatrix} \tag{9}$$

$$F_2 = \begin{bmatrix}0 & 0 & 0 & 0\\ 0 & 0 & 0 & 0\\ 0 & 0 & 0 & \Delta t\cos(\theta_k)\\ 0 & 0 & \Delta t\cos(\theta_k) & -\Delta t v_k\sin(\theta_k)\end{bmatrix} \tag{10}$$

Based on P_k we can also predict the covariance matrix of the state estimate $\bar{P}_{k+1}$ via Eq.(11).

$$\bar{P}_{k+1} = A_k P_k A_k^T + Q_k \tag{11}$$

The state-transition matrix A_k is defined in Eq.(12).

$$A_k = \begin{bmatrix}1 & 0 & \Delta t\cos(\theta_k) & -v_k\Delta t\sin\theta_k\\ 0 & 1 & \Delta t\sin(\theta_k) & v_k\Delta t\cos\theta_k\\ 0 & 0 & 1 & 0\\ 0 & 0 & 0 & 1\end{bmatrix} \tag{12}$$

$$Q_k = \begin{bmatrix}0 & 0 & 0 & 0\\ 0 & 0 & 0 & 0\\ 0 & 0 & \Xi^v & 0\\ 0 & 0 & 0 & \Xi_k^\theta\end{bmatrix} \tag{13}$$

The process-noise covariance matrix Q_k consists of the velocity increment $(v_{k+1} - v_k) \sim N(0, \Xi_k^v)$ and the increment of the angle $(\theta_{k+1} - \theta_k) \sim N(0, \Xi_k^\theta)$. By including the control inputs for v and θ as noise, the magnitudes of Ξ_k^v and Ξ_k^θ are likely larger than would otherwise be required, but with the benefit of a method that is independent of communication with the robot.

In *update steps* (performed when measurements are available) we correct the predicted state estimation based on the measurements. The update step contains the following computations.

$$\begin{aligned}S_{k+1} &= C\bar{P}_{k+1}C^T + R\\ K_{k+1} &= \bar{P}_{k+1}C^T S_{k+1}^{-1}\\ \hat{X}_{k+1} &= \bar{X}_{k+1} + K_{k+1}(Z_{k+1} - C\bar{X}_{k+1})\\ P_{k+1} &= (I - K_{k+1}C)\bar{P}_k\end{aligned} \tag{14}$$

The covariance matrix of the measurement noise, R, is given below.

$$R = \begin{bmatrix}W_x & 0\\ 0 & W_y\end{bmatrix} \tag{15}$$

2.2 Variation of Orientation Covariance

As discussed above, it is likely that increments of θ will be larger as $v(t) \to 0$. For this reason instead of only considering variance Ξ_k^θ constant, we also consider the variance as a function of velocity v, i.e., $\Xi_k^\theta = \Xi_k^\theta(v_k)$.

In Eq.(11) and Eq.(13) above, the process noise covariance matrix Q_k, and more specifically Ξ_k^θ, is noted to vary from step to step, and as such must be re-evaluated after each update. Here we denote the dependence of $[Q]_{44}$ on v, such that it achieves its maximum value for $v = 0$ and decreases monotonically to $[Q]_{44} = 0$ at $v = \bar{v}$. The proposed function defining the relationship between Ξ_k^θ and v, given in Eq.(16), is based on the observed empirical histogrammatic correlation between v and $\Delta\theta$ over several data sets.

$$\Xi_k^\theta(v_k) = \arccos^2[(\frac{v_k}{\bar{v}})^4] \tag{16}$$

This function requires one tuning parameter, $\bar{v}$. After performing several optimization iterations using the Matlab®Optimization Toolbox, we observed that the normalization parameter correlates well with the histogrammatic peak of v for a given trajectory. It is clear, however, that for such a definition of $\bar{v}$, v_k will almost certainly exceed $\bar{v}$ at times, in which case the $\arccos$ function returns non-real values. Protections have thus been implemented in the software to ensure real values. The practical implication is that $|v| \geq \bar{v} \to \Xi_k^\theta(v_k) \equiv 0$.

Figure 1: Overhead view of Khepera-II arena. Image taken from Cognex Insight 5400 machine vision sensor, showing several Khepera-II robots with unique identifier IDs (for truth measurements).

3 Experimental Data

The method of orientation estimation described in this paper has been implemented in the Khepera-II testbed within our experimental laboratory [25]. The testbed, shown in Figure 1 and Figure 6 has been constructed for the purpose of studying and validating swarm- and cooperative-robotics control methodologies in the presence of true sensor noise, and communication uncertainties and limitations.

Experimental data sets with the Khepera-II robots, SICK LMS-400 LADAR sensors, and the Cognex InSight 5400 vision system have been collected to provide real inputs to the algorithms. The data thus includes real-world corruption such as dropped or misread measurement packets, non-real values, noise due to environmental conditions, and sensor noise.

Data was gathered via the Cognex InSight 5400 vision system with a single robot present within the arena, moving under the Braitenberg obstacle avoidance algorithm built in to the Khepera-II standard library. The implementation is a variant of Braitenberg's Vehicle 3b, also called *Like* [26]. The resulting trajectories are non-deterministic and depend strongly on the initial orientation relative to the arena geometry, as well as on the variation among the on-board IR proximity sensors. Five data sets were collected with the robot moving in this manner. One of these sets was chosen arbitrarily to tune the parameter $\bar{v}$. The training trajectory is shown in Figure 2. The remaining trajectories are plotted in Figure 3.

These initial data sets were gathered using distinct identifier discs atop the robots (as visible in Figure 1) such that direct measurement of robot orientation would be possible and available for comparison. These sets were used to validate methods without the concerns of processing time for the vision system. These data sets contain only data from the Cognex vision system. Four additional data sets

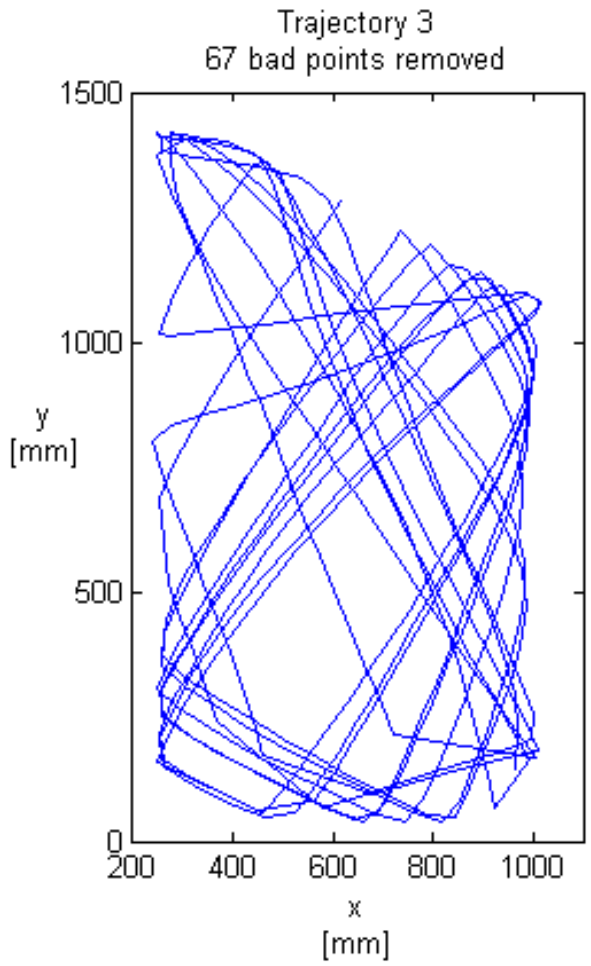

Figure 2: The robot trajectory used to find the optimal value of $\bar{v}$. The figure excludes invalid measurements, which are identified in the algorithm and treated as 'skipped' measurements.

were taken with a stationary robot in different locations to quantify the sensor noise covariances (i.e., measurement noise R), including evaluation of whether the sensor error is a function of location within the arena. For the Cognex vision system, location does not significantly affect the noise covariance; the SICK LADAR sensor noise does vary significantly across the field of view. Results are given below for the data collected by the Cognex vision system.

4 Experimental Results

Simulations conducted with the above described data sets as inputs allowed the tuning of model parameters, as the estimated states could be directly compared to the measured states. The relationship between the noise intensity Ξ_k^θ and estimated velocity proposed in Eq.(16) has been optimized. The tuning parameter for this velocity-dependent noise profile was optimized under an arbitrarily chosen trajectory set from the single-robot data. For a fair and legitimate com-

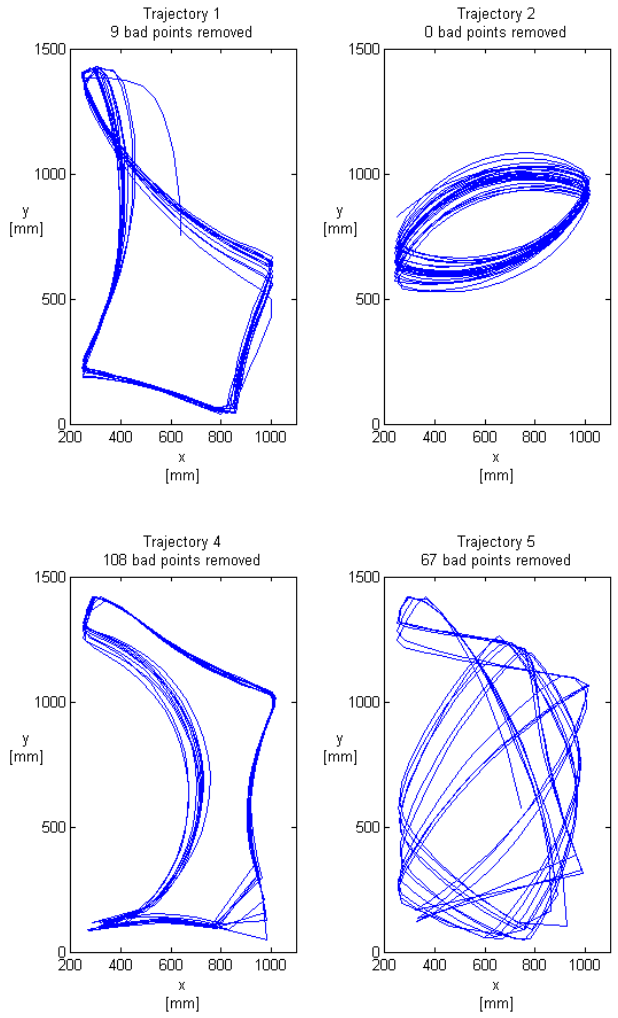

Figure 3: Four of the five measured trajectories. The figures exclude invalid measurements, which are identified in the algorithm and are treated as 'skipped' measurements.

parison, the fixed-noise covariance magnitude was also optimized under the same trajectory. The varying-noise function is plotted in Figure 4, with the fixed-noise value also plotted for comparison. As seen in the plot, the optimized parameter is $\bar{v} = 756$mm/s.

The relative performance of the varying-noise model compared to the constant-noise model was evaluated by comparing the mean squared error between the measured and estimated angle, i.e., $\sqrt{\sum_k (\text{mod}(\theta - \hat{\theta}, 2\pi))^2}$. The modulo function is critical to account for angle-wrapping; i.e., to account for the fact that $\hat{\theta} = \hat{\theta} + 2\pi$. Table 1 gives the scores (RMS error, expressed in radians) for the constant-noise and variable-noise models for each of five trajectories. The greatest score improvement (error reduction) is for Set 3, which was used as the training set for optimizing $\bar{v}$. Figure 5 illustrates the difference between measured and estimated orientation. The measured data is real and includes noise, evidenced by some non-smooth segments.

Table 1:
Estimation error

	constant	varying	%change
Set 1	0.1382	0.1475	6.75
Set 2	0.2212	0.2030	-8.23
Set 3*	0.2168	0.1881	-13.24
Set 4	0.1276	0.1389	8.85
Set 5	0.2155	0.2005	-7.00

Relative performance (RMS angular error, radians) of the varying-noise model compared to the constant-noise model.

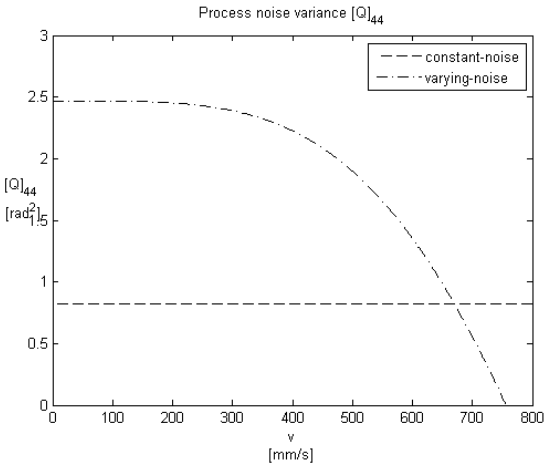

Figure 4: $\Xi_k^\theta(v)$ candidate function.

5 Applicability

This methodology can be applied on similar, differential-driven robot system utilizing position-only feedback. Use of this method has the potential to greatly reduce the sensing requirements in situations where orientation information is desired. For example, for beacon-, *a-priori*-known map-, or time-of-flight-based navigation systems could reduce the number of beacons, features, transmitters, etc., such that only position measurements are required.

In this paper, it is asserted that this estimation method is possible due to the physical constraints of a differential-drive vehicle. However, experiments have been performed only with a single trajectory control method, and thus this claim remains unproven. Continuing experiments and simulations seek to answer the question of whether this method is applicable under other trajectory control paradigms.

These experiments have focused solely on estimation via an external observer, alleviating high-throughput communication of control input by the robot to the observer. If this method is implemented on-board the robot, utilizing its own exteroceptive sensing ability to yield x-y measurements, the control inputs would be available to the estimation algorithm as well, thus significantly reducing the required magnitude of the process noise injected into the

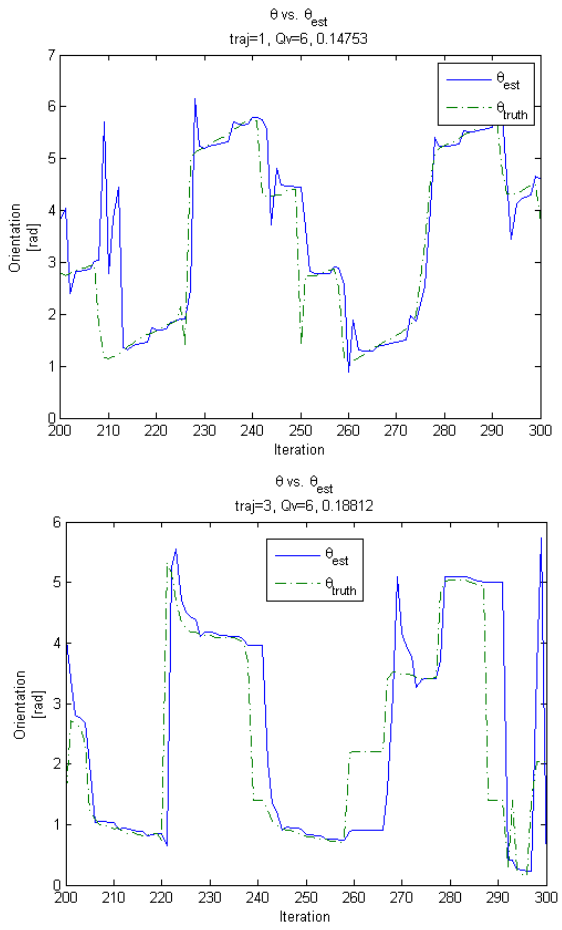

Figure 5: θ_{truth} vs. $\hat{\theta}$ for varying-noise model, trajectory sets 1 and 3. Zoomed in to show detail.

model.

This extension of the method allows the potential of greater scalability with multiple vehicle systems as the sensing and processing requirements are drastically reduced. Furthermore, applications in holonomic estimation and control may be possible. For example, a quadrotor aerial vehicle with 6DOF could exploit a system such as this *if the control input is known*.

6 Conclusion

The method of varying the estimated process noise covariance of the orientation state as a function of velocity proved to work admirably. The errors observed under the varying-noise model were, for three of the five test trajectories, significantly lower than for the constant-noise model. Clearly though, two of the trajectories result in increased estimation error with the varying-noise model. These results are compelling, and suggest that such a varying-noise model, appropriately configured, may be able to reduce estimation error. We continue to study the differences in the trajectories in an attempt to identify cases where use of a noise-

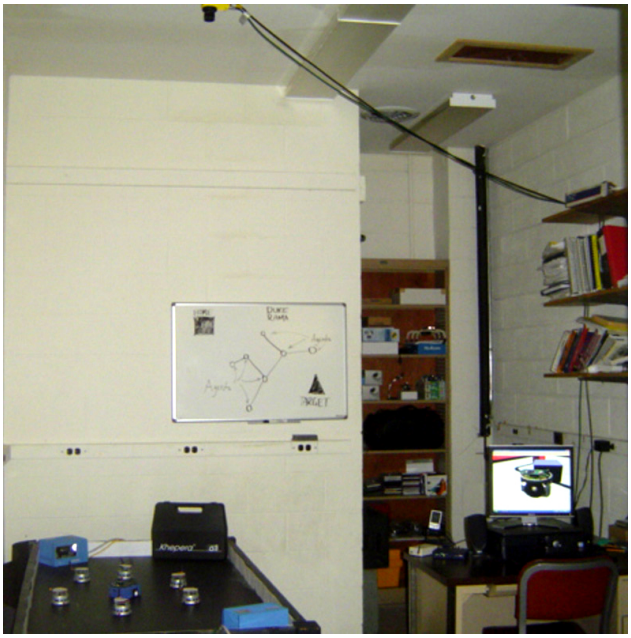

Figure 6: View of the Khepera-II lab space, showing relative locations of Cognex Insight 5400 camera and dual SICK LMS400 ladar sensors.

varying model will be most beneficial. We suspect that the dynamic ranges of the states are critical to the convergence of the estimator; a potential method of evaluating the dynamic ranges of the trajectories has been inspired by the numerical conditioning suggested by Antonelli [6].

7 Acknowledgement

This work was supported by the Army Research Office under grant number W911NF-08-1-0106 titled “Modeling, Analysis, and Control of Swarming Agents in a Probabilistic Framework”.

References

[1] J. Borenstein & L. Feng, Measurement and correction of systematic odometry errors in mobile robots, *IEEE Trans. on Robotics and Automation, 12*(6), 1996, 869–880.

[2] K. S. Chong & L. Kleeman, Accurate odometry and error modelling for a mobile robot. *Proc. IEEE International Conf. on Robotics and Automation (ICRA’97)*, Apr 1997, 2783–2788.

[3] T. D. Larsen, M. Bak, N. A. Andersen, & O. Ravn, Location estimation for an autonomously guided vehicle using an augmented Kalman filter to autocalibrate the odometry. *Proc. FUSION98 SPIE Conf.*, Las Vegas, Jul. 1998.

[4] H.-J. Von der Hardt, R. Husson, & D. Wolf, An automatic calibration method for a multisensor system: application to a mobile robot localization system. *Proc. IEEE International Conf. on Robotics and Automation, (ICRA'98)*, 1998, 3141–3146.

[5] A. Martinelli, N. Tomatis, A. Tapus, & R. Siegwart, Simultaneous localization and odometry calibration for mobile robot. *Proc. IEEE/RSJ International Conf. on Intelligent Robots and Systems (IROS'03)*, Oct. 2003, 1499–1504.

[6] G. Antonelli, S. Chiaverini, & G. Fusco, A calibration method for odometry of mobile robots based on the least-squares technique: theory and experimental validation, *IEEE Trans. on Robotics 21*(5), 2005 994–1004.

[7] S. Murata and T. Hirose, Onboard locating system using real-time image processing for a self-navigating vehicle, *IEEE Trans. on Industrial Electronics, 40*(1), 1993, 145–154.

[8] K. Kato, H. Ishiguro, & M. Barth, Identifying and localizing robots in a multi-robot system environment. *Proc. IEEE/RSJ International Conf. on Intelligent Robots and Systems (IROS'99)*, 1999, 966–971.

[9] J. Leonard and H. Durrant-Whyte, Mobile robot localization by tracking geometric beacons, *IEEE Trans. on Robotics and Automation, 7*(3), 1991, 376–382.

[10] C.-C. Tsai, H.-H. Lin, & K.-H. Wong, Laser-based position recovery of a free-ranging automatic guided vehicle. *Proc. IEEE International Conf. on Mechatronics(ICM '05)*, July 2005, 1–6.

[11] H.-H. Lin, C.-C. Tsai, & J.-C. Hsu, Ultrasonic localization and pose tracking of an autonomous mobile robot via fuzzy adaptive extended information filtering, *IEEE Trans. on Instrumentation and Measurement, 57*(9), 2008, 2024–2034.

[12] I. Rekleitis, G. Dudek, & E. Milios, Multi-robot exploration of an unknown environment, efficiently reducing the odometry error. *Proc. International Joint Conf. in Artificial Intelligence (IJCAI)*, 1997.

[13] S. Roumeliotis & G. Bekey, Distributed multirobot localization, *IEEE Trans. on Robotics and Automation, 18*(5), 2002, 781–795.

[14] S. Thrun, Simultaneous localization and mapping. *Robotics and cognitive approaches to spatial mapping* (Berlin / Heidelberg: Springer, 2008), 13–41.

[15] F. Lu & E. Milios, Robot pose estimation in unknown environments by matching 2d range scans, *Journal of Intelligent and Robotic Systems, 18*(3), 1997, 249–275.

[16] C. Stachniss, Exploration and mapping with mobile robots. Ph.D. dissertation, University of Freiburg, Department of Computer Science, April 2006.

[17] S. Se, D. Lowe, & J. Little, Vision-based global localization and mapping for mobile robots, *IEEE Trans. on Robotics, 21*(3), 2005, 364–375.

[18] R. E. Kalman, A new approach to linear filtering and prediction problems, *ASME Journal of Basic Engineering, 82*, 1960, 35–45.

[19] M. Athans, R. Wishner, & A. Bertolini, Suboptimal state estimation for continuous-time nonlinear systems from discrete noisy measurements, *IEEE Trans. on Automatic Control, 13*(5), 1968, 504–514.

[20] D. Jung, J. Heinzmann, & A. Zelinksy, Range and pose estimation for visual servoing of a mobile robot. *Proc. IEEE International Conf. on Robotics and Automation (ICRA'98)*, May 1998, 1226–1231.

[21] S. Hoyt, S. Mckennoch, & L. G. Bushnell, An autonomous multi-agent testbed using infrared wireless communication and localization. Technical Report, Dept of EE, University of Washington, UWEETR-2005-0005, 2005.

[22] T. Chung, V. Gupta, J. Burdick, & R. Murray, On a decentralized active sensing strategy using mobile sensor platforms in a network. *Proc. IEEE Conf. on Decision and Control (CDC'04)*, Dec. 2004, 1914–1919.

[23] L. Slafer, The use of real-time, hardware-in-the-loop simulation in the design and development of the new Hughes HS601 spacecraft attitude control system. AIAA Technical Library, NTIS HC A20/MF, 1989.

[24] W. Jin & X. Zhan, A modified Kalman filtering via fuzzy logic system for ARVs location. *Proc. International Conf. on Mechatronics and Automation (ICMA'07)*, Aug. 2007, 711–716.

[25] G. K. Fricke, D. Milutinović, & D. P. Garg, Sensing and estimation on an experimental testbed for swarm robotics. *Proc. ASME Dynamic Systems and Controls Conf. (DSCC'09)*, to appear Oct. 2009.

[26] V. Braitenberg, *Vehicles: Experiments in synthetic psychology*. (Cambridge, Massachusetts: MIT Press, 1984).